# Antibodies generated against streptococci protect in a mouse model of disseminated aspergillosis[1]

**Rebekah E. Wharton**[2],[*],[+], **Emily K. Stefanov**[*], **R. Glenn King**[*], and **John F. Kearney**[*]

[*]Department of Microbiology, University of Alabama at Birmingham, Birmingham, AL 35294 USA

[+]Department of Pathology, University of Alabama at Birmingham, Birmingham, AL 35294 USA

## Abstract

Invasive Aspergillosis (I.A.) resulting from infection by *Aspergillus fumagatus* (A.f.) is a leading cause of death in immunosuppressed populations. There are limited therapeutic options for this disease and currently no vaccine. There is evidence some anti-A.f. monoclonal antibodies can provide protection against I.A. However, vaccine development has been impeded by a paucity of immunological targets on this organism demonstrated to provide protective responses. Sialylated oligosaccharide epitopes found on a variety of pathogens including fungi and Group B Streptococci (GBS) are thought to be major virulence factors of these organisms facilitating pathogen attachment to host cells and modulating complement activation and phagocytosis. As some of these oligosaccharide structures are conserved across kingdoms, we screened a panel monoclonal antibodies raised against GBS serotypes for reactivity to A.f. This approach revealed that SMB19, a GBSIb type-specific mAb, reacts with A.f. conidia and hyphae. The presence of this antibody in mice, as a result of passive or active immunization, or by enforced expression of the SMB19 heavy chain as a transgene, results in significant protection in both intravenous and airway-induced models of I.A. This study demonstrates that some antibodies generated against bacterial polysaccharides engage fungal pathogens and promote their clearance in vivo and thus provide rationale of alternative strategies for the development of vaccines or therapeutic monoclonal antibodies against these organisms.

## Introduction

Fungal infections involving opportunistic pathogens have increased dramatically in the last 20 years. Although normally harmless, infection by these organisms results in severe diseases in immunocompromised individuals including AIDS patients, as well as those subjected to severe immunosuppressive regimens involved in transplantation or chemo-myeloablation. *Aspergillus fumigatus* (A.f.), the causative agent of invasive Aspergillosis (I.A.), is the most prevalent airborne, opportunistic fungal pathogen that causes life-threatening disease amongst immunosuppressed populations in medical centers worldwide.

Corresponding Author: Dr. John F. Kearney, Office: (205) 934-6557, Fax: (205) 996-9908, jfk@uab.edu.
[2]This research is part of the dissertation research conducted by REW, a pre-doctoral student in the Pathology Graduate Program, University of Alabama at Birmingham, Birmingham, AL 35294.

I.A. results in mortality rates ranging from 40-80% and this disease, already a significant health problem, is likely to become more prevalent due to the lack of effective therapies or vaccines (1). Compounding the serious nature of these infections are increasing rates of immunodeficiencies, overuse of antibiotics, and the emergence anti-fungicide resistant strains.

Thus far, most new therapeutic efforts have been directed towards development of vaccines to induce T cell activation or the production of cytokines, which are thought to be helpful in clearing fungal infections (2, 3). However, active vaccination is problematic in the case of immunosuppressed individuals, in particular those with compromised T cell immunity. Although many fungal cell wall components elicit antibody responses, few of these induced antibodies provide protection in fungal infection models (4, 5). In addition, the observation that serum anti-A.f. antibody does not correlate with clinical improvement and that that μMT mice are resistant to A.f. infections (6) have had a negating effect on efforts to generate vaccine strategies to induce protective antibody responses. Although monoclonal antibodies (mAbs) directed against β-glucans, components of fungal cell walls (7, 8), and to an undefined glycoprotein (9) have been shown to provide protection in A.f. infection models, to our knowledge protection elicited by other antibody-associated A.f. epitopes has not been reported. Additionally, passive antibody treatment alone or in combination with cell-mediated immunotherapy or antifungal reagents has the potential to provide effective therapy in those with impaired immunity or those about to undergo immunocompromising treatments. Despite the few studies that show certain antibodies to fungal cell wall components, especially polysaccharides (PS), can provide protection (10). the lack of knowledge of the nature of crucial fungal targets and host effector mechanisms involved in protection by anti-A.f. antibodies has hampered the development of an effective anti-A.f. vaccine. Previous attempts to develop vaccines against fungal infections have concentrated on the products made or released by the fungi themselves, however some but not all of these components have low intrinsic antigenicity or the ability to dampen host responses (4, 5).

In this study we show that a mouse mAb to GBS, type Ib (GBSIb), SMB19 (IgM,κ), reactive with the oligosaccharide sialyl-lacto-N-tetraose (s-LNT) epitope also binds to A.f. conidia and hyphae and is protective in inhalation and intravenous models of Aspergillosis. Because PS-tetanus toxoid conjugate vaccines, which provide protective antibody responses against infection of multiple Group B streptococci, have been developed and used successfully in human clinical trials for some years (18), the results we have obtained in these mouse models suggest that GBS-PS conjugate vaccines may be repurposed to develop successful vaccines against A.f. and other clinically important human fungal pathogens.

## MATERIALS AND METHODS

### Mice

Eight to twelve week old C57BL/6J, B6.129P2-$Tcrb^{tm1Mom}$ $Tcrd^{tm1Mom}$/J (TCRβ/δ−/−), B6.129S2-$Igh$-$6^{tm1Cgn}$/J (μMT) and $Ncf1^{tm1J}$/J ($p47^{phox}$−/−) mice were purchased from Jackson Laboratories (Bar Harbor, ME) and bred and housed in pathogen-free animal facilities. VH J558 Tg mice were generated using the rearranged VDJ from a J558 IgG3 hybridoma previously described (11). C3−/− mice, and C5−/− mice, generated from

backcrossing the DBAJ2 mice onto the C57BL/6 background for over 8 generations, were both gifts from Dr. Scott Barnum, UAB. VH SMB19 Tg mice were generated using the rearranged genomic DNA VDJ from the SMB19 hybridoma (12), NCBI Accession sequence BN000872. Genomic DNA was amplified using the primers 5′-CGCCTGGATGGACTGGGTCCGC-3′ and 5′-GCTTCTAATTTCAGCAACCCAC-3′. The PCR product was cloned into the previously described KC9 construct (13) at NcoI and BamHI restriction sites and VH SMB19 Tg mice generated as described previously for the VH81× Tg mouse(13).

## Microorganisms and Monoclonal antibodies

*Aspergillus fumigatus* (strain 13073) and isolates of *Aspergillus niger* (strain IMI 31274) and *Aspergillus flavus* (strain CBC B5107), all purchased from ATCC, were cultured on potato dextrose agar (Fisher) plates at 37°C for 5 days then harvested as described (16) in PBS, counted on a hemocytometer, and stored at 4°C. Group B streptococci, (strain names in parenthesis), GBS–Ib (H36B), GBSIa, GBSII (18RS21), and GBSIII (COH1) used in flow cytometry experiments and vaccinations were gifts from Dr. David Pritchard (UAB). GBS used for vaccines were grown to log phase, washed 3 times, and fixed overnight in 1% PFA at 4°C. mAbs specific for these GBS serotypes, α-1,3 glucan, and the anti-idiotype antibody, SMBi26 against SMB19 are described, together with methods of purification and quality control, in Supplementary Table 1.

## Biacore Analyses

Biacore T200 (UAB Multidisciplinary Molecular Interaction Core) was used to assess the binding of SMB19 to GBS Ib capsular PS. Purified biotinylated GBSIb capsular PS was captured on a SA (Streptavidin) Sensor Chip for the Biacore T200. After washing in a running buffer containing 3mM EDTA to chelate $Ca^{++}$, SMB19, was injected over the SA-captured GBSIb capsular PS Chip surface in the presence of 0.9mM calcium chloride (red) or 3mM EDTA (green) (Fig 2) in the running buffer at concentrations ranging from 0.68 μg/ml to 50 μg/ml. Sensorgrams (binding curves) were obtained and displayed simultaneously.

## Treatment of A.f. with Phospholipase C

A.f. conidia were germinated for 18 hours in RPMI in a Petri dish at 37C, harvested and washed 2 times in PBS (20 min, 2000 rpm) and one time in PI-PLC enzyme buffer (50mM Tris HCl, 150mM NaCl, 5mM EDTA in dH20, pH 7.4). AF were then resuspended in 1ml enzyme buffer containing 0.4 units of phosphatidylinositol-specific, Phospholipase C, (MP Biomedicals, Solon, OH) and incubated for 60 min at 37C. The A.f. preparation was then washed 2× in PBS and stained with 0.5ug mAb for 30min, followed by goat-anti-mouse IgM FITC (SBA, Birmingham, AL) and analyzed on a FACSCalibur. The no PI-PLC group was treated the same except for the addition of the enzyme. Cleavage of GPI-linked Thy 1 on mouse T cells was used as a control for the enzyme function

### Flow cytometry

For A.f. flow cytometry staining, A.f. conidia were cultured in 50 ml conical tubes for 12 hours at 37°C in RPMI 1640 to form hyphae. Then, paraformaldehyde (PFA)-fixed GBS or live resting A.f. conidia or hyphae were blocked at 4°C in 1% bovine serum albumin (BSA) then incubated with purified anti-GBS type-specific IgM mAbs. Polyclonal goat anti-mouse IgM coupled to Cy5 (Southern Biotech, Birmingham, AL) was used to detect binding by flow cytometry. All GBS type-specific mAbs were gifts from Dr. David Pritchard, UAB. IgM binding to A.f. was analyzed on a FACScalibur (Becton-Dickinson, Mountain View, CA) and FlowJo software.

For SMB19 Tg mouse characterization flow cytometry, spleen, bone marrow, mesenteric lymph nodes, and peritoneal cavity lavage cells were removed from SMB19 Tg or C57BL/6J mice. Cells were counted, blocked with anti-FcRγ (Ab93), and stained with the antibodies listed below. Phycoerythrin (PE) anti-B220 (RA3-6B2), PE-Cy7 anti-B220 (RA3-6B2), PE anti-AA4.1, fluoresceinated (FITC) anti-CD23 (B3B4), pacific blue (PB) goat anti-IgM, biotin anti-CD23 (B3B4), APC-Cy7 anti-CD19 (1D3), FITC anti-CD5 (53-7.3), and PE anti-CD11b (M1/70), and Alexa Fluor-488 anti-CD21 (7G6) were purchased from BD Pharmingen (San Diego, CA). SMBi26, rat anti-SMB19 idiotype hybridoma, was generated using previously described methods (14). Cell frequencies were analyzed on a Becton Dickinson LSRII flow cytometer.

### Vaccinations

8-10 week old C57BL/6J mice were vaccinated intravenously (i.v.) with either $1\times10^8$ PFA-fixed GBSIb, or GBSII or PBS vehicle. Six days after vaccination, mice were infected with a lethal dose of A.f. conidia i.v. and monitored for survival. Mice were euthanized with $CO_2$ when they appeared moribund according to UAB ARP provisions.

### I.v. Infections with A.f.

For experiments involving passive antibody transfer. C57BL/6J, TCRβ/δ−/−, C3$^{-/-}$, or C5 deficient mice were given 200 μg of SMB19, SIbD2, or A16 intraperitoneally (i.p.) then immediately infected i.v. with A.f. conidia and monitored for survival. In experiments involving a neutropenic model of I.A. in WT mice, C57BL/6J mice were given 200 μg of anti-Ly-6G (1A8 clone hybridoma a gift from Dr. Thomas Malek) i.p. 1 day prior to infection with A.f. and in some experiments, another 2 days post infection with A.f. On day 0, mice were passively administered 200 μg SMB19 or SIbD2 i.p., then immediately infected A.f. i.v. and monitored for survival. Endpoints for these experiments were gauged as mouse unresponsiveness to touch for >2 hrs (this includes un-controlled rolling over in the cage, but not responding when touched). Mice were euthanized with $CO_2$ when they appeared moribund. In experiments involving a I.A. in Tg mice, all SMB19 Tg, J558 Tg, μMT, or C57BL/6J mice were infected with $2\times10^6$ A.f. conidia i.v. and monitored for survival. Mice were euthanized with $CO_2$ when they appeared moribund.

### I.t. Infections with A.f.

In experiments involving a neutropenic model of i.t. A.f.infection, C57BL/6J, SMB19 Tg and J558 Tg mice were given 200 μg of anti-Ly-6G (1A8 clone hybridoma a gift from Dr. Thomas Malek) i.p. 2 hours prior to infection with i.t. infection with $2\times10^7$ A.f. $Ncf1^{m1J}/J$ ($p47^{phox}$–/–) mice were infected i.t. with $10^5$ A.f. and 50μg SMB19 or control (No Ab) i.t. I.t infections were pre-formed as described in (16). Mice were monitored for survival. Mice were euthanized with $CO_2$ when they appeared moribund.

### Inhibition ELISA

A.f. conidia were germinated in a Nunc 96-well Maxisorp plate in DMEM supplemented with 10% FCS for 8 hours at 37°C in a $CO_2$ incubator, then dried overnight at 37°C. Wells were washed with PBS and blocked with 1% BSA. 250 ng/ml SMB19 in 1% BSA was then added to each well along with 1 mg/ml of s-LNT or LNT (Carbosynth, Berkshire, UK) or 0.5 mg/ml GBSIb polysaccharide (gift from Dr. Dennis Kasper, Harvard University), or α-1-3 dextran (a gift from Dr. A. Jeanes) in Dulbecco's PBS (DPBS). After 2 hours incubation at 37°C, the wells were washed with PBS and incubated with goat anti-mouse IgM-AP (SBA, Birmingham, AL) for 1 hour. Plates were then washed with PBS, developed with AP substrate buffer, pH 9.8, stopped with 5N NaOH, and O.D. measured at 405 nm on a BMG Labtech microplate reader (Cary, NC).

### GBSIb type-specific PS and GBSII type-specific PS ELISAs

Nunc 96-well maxisorp plates were coated with poly-L-lysine for 30 minutes at room temperature. Purified capsular PS from GBSIb or GBSII was diluted in DPBS and added to each well and dried overnight at 37°C. Wells were washed 3 times with PBS, and blocked with 1% BSA. Mouse anti-sera was then diluted and added to each well, then incubated for 2 hours at 37°C. Alkaline phosphatase (AP) goat anti-mouse IgM (Southern Biotech, Birmingham, AL) was used as the secondary antibody and plates were developed with alkaline phosphatase buffer, pH 9.8. O.D. was read at 405 nm on a BMG Labtech microplate reader (Cary, NC).

### ELISA assays for detection of the SMB19 idiotype, α−1,3 dextran, and IgM[a]

Costar 96-well plates were coated with 1 μg/ml (SMBi26) anti-idiotype antibody to SMB19, α−1,3 dextran, or anti-IgM[a] (RS3.1) in PBS overnight at 4°C. Plates were then washed with PBS three times and blocked with 1% BSA. Mouse sera were diluted in PBS, added to each well and plates were incubated for 2 hours at 37°C. AP goat anti-mouse IgM (Southern Biotech, Birmingham, AL) was used as the secondary antibody and plates were developed with alkaline phosphatase buffer, pH 9.8. O.D. was read at 405 nm on a BMG Labtech microplate reader (Cary, NC).

### Immunofluorescence Tissue Section Analysis

Spleens were collected from mice, frozen in OCT, and cryostat sections were fixed in acetone, frozen, and stained with Alexa Fluor 350 anti-MOMA-1, Alexa Fluor 647 anti-IgM[a] (RS3.1), Alexa Fluor 488 anti-SMB19 idiotype (SMBi26), and PE anti-CD4 (RM4-5, BD Pharmingen) and PE anti-CD8 (53-6.7, BD Pharmingen). Brain and kidney sections

from SMB19 Tg, J558 Tg, µMT, and C57BL/6 mice were frozen and stained with Alexa Fluor 647 anti-Ly6G (1A8), Alexa Fluor 555 anti-CD11b (M1/70), Alexa Fluor 488 anti-β–1-3 glucan (a gift from Dr. M. Feldmesser), and biotin rabbit anti-laminin (NB300-144) (Novus Biologicals, Littleton, CO). Biotinylated anti-laminin was visualized with Alexa Fluor 350 streptavidin (BD Pharmingen, San Diego, CA).

### Quantitative PCR analysis

Brain and kidney DNA was extracted from SMB19 Tg, J558 Tg, µMT, and WT C57BL/6 mice using the DNeasy Blood and tissue kit (Qiagen, Hilden, Germany). Samples were processed and primers used as described previously (15) prior to analysis on a Biorad IQ5 RT-PCR machine. Results are expressed as A.f. conidial equivalents / g tissue.

### A.f. microscopy analysis

A.f. conidia were diluted in RPMI 1640 and seeded on glass slides. Slides contained resting A.f. conidia or A.f. that were germinated for 8 hours and fixed in 95% ethanol at 4°C. Slides were washed with PBS, blocked with 1% BSA, and stained with AlexaFluor-555 SMB19 and AlexaFluor 488 anti-β–1-3 glucan (Clone 744, IgM,κ gift from Dr. Marta Feldmesser) (1), and mounted with DAPI fluoromount. Slides were analyzed using a Leitz DMRB fluorescent microscope.

### Cytokine analysis

Sera from SMB19 Tg, J558 Tg, µMT, and C57BL/6J mice were collected at various time points before and after infection with A.f. Sera were diluted 3 fold and processed using the Milliplex Mouse Cytokine/Chemokine kit (Millipore). Prepared serum samples were run on the Luminex MAGPIX system and results analyzed on Milliplex Analyst software.

### Statistical analysis

Statistical comparisons were performed using Prism 4.0 software (GraphPad). Data with three or more groups were analyzed by a one-way ANOVA test followed by post hoc analysis, whereas data with two groups were analyzed by a two-tailed unpaired t test to determine whether overall statistically significant differences existed. For survival curves, statistical analysis was performed using the Mantel-Cox Log-rank test. Statistically significant results were described by a $p$ value of *<0.05, ** <0.01, ***<0.001.

## RESULTS

### Monoclonal antibodies to the GBSIb capsular polysaccharide bind A.f. hyphae and conidia

We found in recent surveys that certain mAbs, which recognize components from a variety of bacterial species, also bind to A.f. at multiple stages of its life cycle (16). In this analysis, we observed that a previously described mouse mAb, SMB19, bound to A.f. conidia (0 hr) and hyphae (12 hr) of A.f. as detected by flow cytometry (Fig 1A). and fluorescence microscopy. [16] This mAb has been shown previously to bind to a sialylated oligosaccharide, s-LNT associated with the capsular polysaccharide of GBSIb (12). Other mAbs to members of this streptococcal group including GBSIa (SIaE7), GBSII (SIIF5C4),

GBSIII, (SIIIV18), and desialylated GBSIb (SIbD2) (described in supplementary Table 1) do not bind either A.f. conidia or hyphae by flow cytometry (Fig 1A), although all mAbs bind to their respective type specific polysaccharides expressed by the cognate serotype of GBS bacteria (Fig 1B). The binding of SMB19 was notably brightest at the tip of the germination tube and on outgrown hyphae (Fig 1C). Similar SMB19 reactivity was observed with *Aspergillus flavus* and *niger* (supplementary Fig 1A-B).

### Fine specificity and Ca$^{++}$ dependent binding of SMB19 to the target oligosaccharide

The terminal oligosaccharides that define the type-specific capsular PS of GBS are known and are shown in Fig 2A for types Ia, Ib, II, and III. SMB19 binding to its target is highly specific since the capsular PS expressed by GBSIb, which differs from that of GBSIa and the others by having a $\beta1\rightarrow3$ instead of the more common $\beta1\rightarrow4$ Gal-GlcNAc linkage (Fig 2A). Additionally, SMB19 does not react with the desialylated form of GBSIb, which is associated with the oligosaccharide lacto-N-tetraose (LNT) (12). Inhibition of SMB19 binding to A.f. with either s-LNT or GBSIb purified capsular polysaccharide (Ib PS), but not LNT or α-1,3-dextran (DEX) confirms that SMB19 binds a similar epitope to that found on GBSIb (Fig 2B, 2C). In addition, surface plasmon resonance analysis was used to confirm previous observations (12) that the binding of SMB19 to the purified GBSIb capsular PS is highly dependent on the presence of calcium (Fig 2E). Treatment of A.f. hyphae with phosphoinositidyl phospholipase C (PI-PLC) to cleave GPI-linked proteins ablated SMB19 binding whereas 1-21 (anti-α-1,3 glucan) binding was unaffected (Fig 2D).

### Passive transfer of purified SMB19 mAb and vaccination with GBSIb improves survival in a mouse model of disseminated I.A.

Since SMB19 binds to A.f. conidia and hyphae, we determined if this antibody would protect in a mouse model of disseminated I.A. Purified SMB19 (anti-GBSIb), SIbD2 (anti-desialylated GBSIb), or A16 (anti-α-1,3 glucan) were passively administered intraperitoneally (i.p.) to naïve C57BL/6J mice immediately before infection with 2×LD$_{50}$ A.f. conidia i.v. Approximately ~75% of mice that received SMB19, but only 10-30% of mice that received either SIbD2 or A16 survived 60 days after infection (Fig 3A). There were no significant differences in protection between mice that received SIbD2 or A16. I.p. injection of SMB19 revealed that this IgM mAb has an *in vivo* half-life of approximately 2 days (Fig 3B), similar to that found for other IgM antibodies. These results indicate that a single treatment with GBSIb PS-specific SMB19, but not SIbD2 specific for the desialylated GBSIb PS or A16 specific for A.f.-expressed α-1,3 glucans, improves survival against disseminated I.A.

The significant protection provided by passive administration of SMB19 suggested that anti-GBSIb responses, as a result of immunization with GBS-PS would protect mice from A.f. challenge. In order to determine if the antibody response following vaccination is sufficient to replicate the protection observed in passive transfer experiments, and to determine if a protective response is specific to the GBSIb-PS vaccine, C57BL/6J mice were vaccinated i.v. with GBSIb, GBSII or administered PBS. Six days following vaccination, at the predetermined peak of the anti-GBS antibody response, mice were infected i.v. with a lethal dose of A.f. conidia. PBS-treated and GBSII-immunized mice died within ~15 days,

whereas ~50% of GBSIb vaccinated mice survived 60 days (at which point the experiment was ended) (Fig 3C). Thus, GBSIb vaccination significantly prolonged survival compared to PBS sham or GBSII immunized controls indicating that the protection induced is specifically associated with GBSIb vaccination. In GBSIb immunized mice, there was an increase in GBSIb type-specific IgM Ab, in addition to that of the SMB19 idiotype. In contrast, mice vaccinated with GBSII had ~100 μg/ml of GBSII-reactive serum antibody, but very little GBSIb-specific or SMB19 idiotype positive antibody (Fig 3D-F). These results indicate that immunization of mice with GBSIb, but not GBSII promotes survival in ~50% of mice for 60 days after A.f. infection. Furthermore, this protection is associated with increased levels of anti-GBSIb Abs and specifically SMB19 Id+ antibody.

### SMB19 transgenic mice are significantly protected against disseminated I.A.

We have previously observed that passively administered IgM antibody has a limited half-life and levels of antibody to GBSIb peaks at ~7 days after immunization and then subsides. To circumvent the transient nature of the Anti-PS response in mice, we utilized a transgenic mouse expressing the SMB19 heavy chain (characterized in (supplementary Fig 2). In this model, SMB19 idiotype-positive antibody is constitutively maintained at ~10-fold higher levels than in C57BL/6J mice. Additionally, previous studies using μMT mice which lack functional B cells suggested that B cells and antibodies may increase the susceptibility of mice to A.f. infection (6). To address these issues and further investigate the protective role of SMB19 in I.A., we infected SMB19 IgH transgenic (SMB19 Tg), μMT, J558 IgH transgenic (J558 Tg), or C57BL/6J mice with a lethal dose of A.f. conidia i.v. SMB19 Tg mice were highly protected compared to C57BL/6J, μMT mice, or J558 Tg mice (Fig 4A). Interestingly, in contrast to previous reports, μMT mice rapidly succumbed to A.f. infections at similar frequencies to C57BL/6J mice. Additionally, J558 Tg mice, which maintain high levels of antibodies specific for α-1,3 glucan (Fig 4D), a major component of the A.f. cell wall, were not protected compared to C57BL/6J mice. Although C57BL/6J mice and J558 Tg mice both have similar levels of GBSIb PS-binding serum IgM as SMB19 Tg mice, SMB19 idiotype antibodies are significantly lower in these mice. As observed in the GBS vaccination studies described above, the increased levels of SMB19 Id-bearing IgM was significantly correlated with protection in this model of I.A. (Fig 4B-C).

In J558 Tg mice, the observed anti-GBSIb antibodies likely arose from B cells bearing endogenous Ig gene rearrangements. As expected, μMT mice did not have detectable levels of serum immunoglobulins. These results, in conjunction with the protection afforded by purified SMB19 mAb, further indicate that not all polyclonal GBSIb-reactive antibodies provides protection in this model of I.A. (Figure 4B) Instead, a particular subset of antibodies, including those of the SMB19 idiotype that is responsible for the protection observed. Importantly, J558 Tg mice, which express antibodies to a major A.f. cell wall component, are as susceptible as C57BL/6J and μMT mice to A.f. infection.

Since cytokines have been associated with both enhanced susceptibility or resistance to I.A., we analyzed cytokine levels in the sera of each of these groups of mice immediately before, and at 4 and 7 days post infection with A.f. SMB19 Tg mice had significantly lower levels of granulocyte proliferation and survival cytokines G-CSF and GM-CSF, which have been

previously associated with protection against I.A. Additionally, none of the groups of mice analyzed had significantly different levels of Th1 or Th2 cytokines previously associated with protection or susceptibility to I.A., including IL-4, IL-5, IL-10, IL-2, and IFN-γ (Supplementary Fig 3). Taken together, these data show that antibody-mediated protection in this model of I.A. differs mechanistically from protection reported in other systems.

## SMB19 Tg survival correlates with decreased A.f. fungal burden and neutrophil infiltrates in the brain and kidneys

Because SMB19 Tg mice demonstrated significantly higher survival rates following challenge with A.f. than, WT C57BL/6J, μMT or J558 Tg mice, we sought to determine whether this protection correlated with decreased fungal burden in the tissues affected during A.f. pathogenesis. It has previously been reported that brain and kidneys are the major tissues damaged during this A.f. infection model (15), therefore we analyzed both tissues by immunofluorescence and quantitative PCR following A.f. infection. Immunofluorescence analysis revealed that SMB19 Tg mice had significantly fewer A.f. lesions in brain (Fig 5A-E) and kidneys (Fig 5G-K) compared to C57BL/6J, μMT, or J558 Tg mice 4 days after i.v. infection. There were no detectable A.f.-containing lesions in brain or kidney tissue sections from mice that survived 60 days post infection. Furthermore, immunofluorescence analysis showed that A.f.-containing lesions in the brains of C57BL/6J and μMT mice were filled with leukocyte infiltrates including CD11b and Ly-6G positive neutrophils. In contrast, A.f. lesions were undetectable in tissues from most SMB19 Tg mice 4 days post infection. The few lesions observed were surrounded by cells weakly expressing CD11b, but negative for Ly-6G (Fig 5D and 5J). None of the SMB19 Tg mice had visible lesions of A.f. in liver or spleen (data not shown). To more accurately access the global fungal burden within these mice, Quantitative PCR for A.f. genomic DNA was performed. This analysis confirmed that SMB19 Tg mice had less fungal burden in their brain (Fig 5F) and kidney (Fig 5L) than WT C57BL/6J, μMT, and J558 Tg mice. These data show that the survival of SMB19 Tg mice infected with A.f. correlates with a decreased fungal burden and fewer neutrophil infiltrates in tissues known to be damaged as a result of fungal outgrowth following i.v. infection of mice with A.f.

## Neutrophil—depleted SMB19 Tg mice and Ncf1[m1J/]J mice administered SMB19 i.t. are protected after i.t. A.f infection

Although intravenous infection with A.f. conidia may rarely occur, the most common route of disseminated infection in immunodeficient patients is by the inhalation of conidia. Because neutrophil insufficiency as a result of myeloablation is a major risk factor for susceptibility to I.A., we utilized a model of infection that renders mice transiently neutropenic. SMB19 Tg, J558 Tg and wt C57Bl/6J mice were given one i.p. injection of neutrophil-depleting anti-Ly6G mAb, 2 hours before i.t. infection with A.f. This dose of anti-Ly-6G is sufficient to maintain neutropenia over the course of 3-4 days post injection. After mice were confirmed to be neutropenic (Fig 6A), these three groups of mice were infected intratracheally with $2.5 \times 10^7$ A.f. conidia and their survival monitored. As seen in Fig 6B, SMB19 Tg mice were highly protected against infection compared to the C57Bl/6J and J558 Tg mice. This reduced susceptibility of SMB19 Tg mice to I.A. is, similar to that observed in the i.v. model (Fig 4). In a separate model we used Ncf1[m1J/]J mice, which

harbor a NADPH oxidase mutation resulting in an impaired intracellular killing mechanism rendering these mice highly susceptible to A.f. infection by inhalation. Ncf1$^{m1J}$/J mice were challenged i.t. with $1\times10^5$ A.f. conidia alone (black) or in combination with 50μg of SMB19 (green) and monitored for survival. As can be seen in Fig 6C, 80% of mice treated with SMB19 survived 11 days after infection, a time at which all control mice had succumbed to infection. Additionally, 20% of antibody treated mice survived through day 20. The results of these experiments differ from the i.v. model of I.A. in which passive SMB19 administration failed to significantly protect transiently neutropenic mice. In this case, mice passively immunized with SMB19 died at the same rate as unimmunized C57BL/6J mice within the first seven days. These observations indicate that SMB19's mechanism of protection in the i.v. I.A. model is at least partially dependent on neutrophil activity (Supplementary Fig 1C). Protection evident after 7 days may be a result of the combined activity of SMB19 antibody with recovering neutrophils since there was still ~25 μg/mL of SMB19 present in sera of passively transferred mice at this time (Fig 3B). To determine the role of complement components in the protection observed by passive immunization with SMB19, we passively transferred SMB19 or isotype control mAbs i.p. to C3$^{-/-}$ mice then immediately infected them i.v. with a lethal dose of A.f. conidia. There were no differences in survival of C3$^{-/-}$ mice that received SMB19 or isotype control mAbs (Supplementary Fig 1D). C5$^{-/-}$ mice treated with SMB19 were as resistant to A.f. infection as were SMB19-treated C57BL/6J (data not shown). These data suggest, early complement components are involved in SMB19-mediated protection in mice, likely by promoting opsonophagocytosis of A.f. and not via formation of membrane attack complexes. Because a large amount of data suggests that T cells are necessary for long-term survival of A.f. infected mice, we next analyzed the role of T cells in SMB19-mediated protectionagainst i.v infection SMB19 or isotype control antibody was administered i.p. to TCRβ/δ$^{-/-}$ mice immediately before i.v. infection with $2\times LD_{50}$ ($2\times10^6$) A.f. conidia. TCRβ/δ$^{-/-}$ mice that received SMB19 mAb are more resistant to infection than the mice that received isotype control mAb (Supplementary Fig 1E). The degree of protection observed in these animals is similar to that of C57BL/6J mice that received SMB19 mAb (Fig 3A). Collectively, these results show that SMB19, when maintained at relatively high levels, endogenously in the Tg mice or passively introduced, provides substantial protection against infection following inhalation of A.f. conidia. These findings contrast with those in the i.v model which indicate that SMB19-mediated protection is dependent on neutrophil and complement activity, but not the activity of T cells.

## DISCUSSION

Antibodies and B cells historically have not been associated with protection in I.A. due to the lack of correlation between A.f. antibody titers and I.A. protection, and partially due to a study demonstrating that μMT mice, which do not make Ab, were less susceptible in comparison to I.A. than WT mice (6). However, recent studies on the role of mAbs in protection against A.f., especially those against β–1,3 glucans (7), have generated new interest in this field. Few studies, however, have identified new epitopes on A.f. that could be targeted therapeutically with mAbs. Our results show that SMB19, a mAb generated against GBSIb, also bound resting A.f. conidia and more strongly to A.f. hyphae. We have

shown that this antibody provides striking protection in both the i.v. infection model and of greater relevance, in an inhalation model of Aspergillosis.

This mAb binds an epitope distinct from the sialic acid-containing capsular PS found on other GBS serotypes, by its preference for the GBSIb type-specific oligosaccharide containing a β–1,3 instead of β–1,4GalNAc-GlcNAc characteristic of the other subtypes. The fact that SMB19 bound preferentially to the tips of A.f. hyphae is particularly interesting since the nascent cell wall of growing hyphae is especially vulnerable to external influences, and as such, is the target site for certain antifungal agents. The observation that binding of SMB19 to its oligosaccharide antigen is calcium dependent, may also have some bearing on SMB19 binding to A.f., since proper outgrowth of fungal hyphal tips relies on high cytoplasmic calcium gradients (17). Dysregulation of these gradients inhibits hyphal growth and disrupts tip morphology. It is possible that SMB19 preferentially binding to A.f. hyphae tips is facilitated by high levels of calcium flux and contributes to the unique protective properties of this antibody.

Passive administration of SMB19 results in significant protection in the i.v. model of infection, in contrast to treatment with A16 which binds α-1,3 glucan, a major cell wall component of A.f. Furthermore, C57BL/6J mice vaccinated with GBSIb, which induces moderate increases of SMB19 idiotype positive antibody, were protected to a greater extent than the mice that received passive antibody. Finally, SMB19 Tg mice, which maintain constitutively high levels of SMB19 idiotype positive IgM, are significantly resistant to A.f. challenge. Although there were similar levels of antibodies to GBSIb-PS in the serum of all groups of mice following immunization, only SMB19 Tg mice expressed high titers of SMB19 idiotype positive antibody. Thus, not all GBSIb PS-reactive antibodies are protective against I.A. but rather the SMB19 or SMB19-like antibody portion of the response is critical in providing protection against A.f. infection. Furthermore, the highly effective protection shown in the SMB19 Tg mice demonstrates that the protection elicited by immunization with GBS1b-PS is not the result of a unique innate immune response primed by that particular organism, and not other GBS serotypes, since the SMB19 Tg mice are protected in absence of immunization. It is also of great interest that J558 Tg mice, which maintain high titers of antibodies against α-1,3 glucans, a major component of the A.f. cell wall, are not protected in this model of A.f. This observation, further highlights the unique role of SMB19 idiotype-bearing antibodies and its target antigen in mediating the observed protection.

Survival of i.v. infected SMB19 Tg mice correlates with decreased fungal load, neutrophil infiltrates, and abscesses containing actively growing hyphae in the brain and kidneys when, compared with infected J558 Tg, C57BL/6J and μMT mice. Rarely, small areas in the brain of SMB19 Tg mice 4 days post infection contained what appeared to be A.f. remnants surrounded by MAC1+ and Ly6G− cells., These cells could be activated resident brain cells such as microglia. This observation suggests that some A.f. conidia penetrated the blood brain barrier and germinated into the hyphal form in SMB19 Tg mice, but their growth was eventually halted by SMB19-mediated killing leaving only non-metabolic hyphal remnants as shown in Fig 5. Additionally, C3$^{−/−}$ mice, in contrast to C57BL/6J mice, are not protected from i.v induced I.A. after passive administration of SMB19. This indicates that

complement activation is, at least in part, responsible for the therapeutic effect of SMB19 antibody. Also of interest is that, contrary to previous studies on C5 in I.A., our C5 deficient mice were no more susceptible to I.A. than WT mice. In this study, we used C5 deficient mice on the C57BL/6J background compared to WT C57BL/6J mice, whereas in the previous study, DBA/2N mice, which are deficient in C5 were compared with CFW mice (18). Differences in these mouse strains could possibly contribute to the differences in survival of A.f. infected mice in these studies, which were attributed to the loss of compliment components. Many studies have implicated T cell immunity as being particularly important in clearing A.f. following infection. We have shown here that that SMB19 antibodies do not depend on T cells for the immediate protection observed in this model of acute A.f. infection.

Our studies of A.f. infections during transiently induced neutropenia indicate that neutrophils are important for protection against I.A. afforded by SMB19 antibodies in mice challenged i.v. Interestingly, however, in two models where neutrophils were transiently depleted or were severely impaired in their bactericidal capacity, SMB19 antibodies were highly protective against infection when conidia were administered into the lung. In the case of the SMB19 Tg mice this protection was highly effective and prolonged. SMB19 co-administration with conidia was nearly as protective in Ncf1$^{m1J}$/J mice, which harbor a defect in NADPH oxidase activity, during the first 11 days following infection. Although many of SMB19 treated mice eventually succumbed to infection, 20% of these mice survived at least 20 days. These results suggest that if the level of SMB19-like antibodies is maintained, it will protect against lethal infection in mice that have severely impaired neutrophil numbers or function, which is commonly associated with Aspergillosis in humans. These results also suggest that the protective effects of SMB19-like antibodies may be provided by different mechanisms in response to airway or parenteral A.f. infection.

There are several additional strategies to pursue regarding the development of SMB19-like antibodies as a potential active or passive therapeutic for patients at risk for I.A. Passive antibody could be combined with other antifungal therapies such as amphotericin B, voriconazole, and caspofungin which are administered as standard treatments for I.A. patients. Amphotericin B and voriconazole target ergosterol synthesis on the A.f. membrane whereas caspofungin targets β-1,3-D-glucan synthase enzymatic activity, which also ultimately affects A.f. membrane synthesis. A recent study showed that mAbs against β-1,3 glucans had a modest inhibitory effect on fungal growth *in vitro*. In limited studies, we found that SMB19 did not appear to have a direct effect on *in vitro* growth of A.f.

In patients with the capacity to mount an antibody response, active immunization is feasible. Additionally, GBS-PS-conjugate vaccines against GBS serotypes I-V have already been developed and validated through phase II clinical trials in humans (19). In preliminary studies of sera from humans immunized with these GBS 1b-conjugate vaccines, we have found that there are both IgM and IgG antibodies that bind in a similar pattern to A.f. conidia and hyphal tips as does SMB19. Furthermore, sera from individuals which received the GBSIb vaccine inhibits SMB19 binding to A.f. These results indicate that GBS-conjugates could be re-purposed for uses as antifungal vaccines in at risk individuals. Our preliminary studies show that SMB19 antibody and these human GBS immune sera also

shows intense staining of *Candida albicans* and *Rhyzopus orzae* during their hyphal growth stages, as well as germinating *Fusarium spp* macroconidia indicating antibodies derived from GBS immunization recognize a common epitope on multiple fungi. Future research will determine whether the induction of SMB19-like antibodies of IgM and IgG isotypes induced by GBS conjugate vaccines are "globally" protective against A.f. and, other clinically relevant fungi (20, 21).

## Supplementary Material

Refer to Web version on PubMed Central for supplementary material.

## Acknowledgements

## References

1. Hohl TM, Feldmesser M. Aspergillus fumigatus: principles of pathogenesis and host defense. Eukaryot Cell. 2007; 6:1953–1963. [PubMed: 17890370]

2. Cutler JE, Deepe GS Jr. Klein BS. Advances in combating fungal diseases: vaccines on the threshold. Nat Rev Microbiol. 2007; 5:13–28. [PubMed: 17160002]

3. Montagnoli C, Fallarino F, Gaziano R, Bozza S, Bellocchio S, Zelante T, Kurup WP, Pitzurra L, Puccetti P, Romani L. Immunity and tolerance to Aspergillus involve functionally distinct regulatory T cells and tryptophan catabolism. J Immunol. 2006; 176:1712–1723. [PubMed: 16424201]

4. Fontaine T, Delangle A, Simenel C, Coddeville B, van Vliet SJ, van Kooyk Y, Bozza S, Moretti S, Schwarz F, Trichot C, Aebi M, Delepierre M, Elbim C, Romani L, Latge JP. Galactosaminogalactan, a new immunosuppressive polysaccharide of Aspergillus fumigatus. PLoS Pathog. 2011; 7:e1002372. [PubMed: 22102815]

5. Latge JP, Kobayashi H, Debeaupuis JP, Diaquin M, Sarfati J, Wieruszeski JM, Parra E, Bouchara JP, Fournet B. Chemical and immunological characterization of the extracellular galactomannan of Aspergillus fumigatus. Infect Immun. 1994; 62:5424–5433. [PubMed: 7960122]

6. Montagnoli C, Bozza S, Bacci A, Gaziano R, Mosci P, Morschhauser J, Pitzurra L, Kopf M, Cutler J, Romani L. A role for antibodies in the generation of memory antifungal immunity. European journal of immunology. 2003; 33:1193–1204. [PubMed: 12731044]

7. Torosantucci A, Chiani P, Bromuro C, De Bernardis F, Palma AS, Liu Y, Mignogna G, Maras B, Colone M, Stringaro A, Zamboni S, Feizi T, Cassone A. Protection by anti-beta-glucan antibodies is associated with restricted beta-1,3 glucan binding specificity and inhibition of fungal growth and adherence. PLoS One. 2009; 4:e5392. [PubMed: 19399183]

8. Rachini A, Pietrella D, Lupo P, Torosantucci A, Chiani P, Bromuro C, Proietti C, Bistoni F, Cassone A, Vecchiarelli A. An anti-beta-glucan monoclonal antibody inhibits growth and capsule formation of Cryptococcus neoformans in vitro and exerts therapeutic, anticryptococcal activity in vivo. Infect Immun. 2007; 75:5085–5094. [PubMed: 17606600]

9. Chaturvedi AK, Kavishwar A, Shiva Keshava GB, Shukla PK. Monoclonal immunoglobulin G1 directed against Aspergillus fumigatus cell wall glycoprotein protects against experimental murine aspergillosis. Clin Diagn Lab Immunol. 2005; 12:1063–1068. [PubMed: 16148172]

10. Blanco JL, Garcia ME. Immune response to fungal infections. Veterinary immunology and immunopathology. 2008; 125:47–70. [PubMed: 18565595]

11. Foote JB, Kearney JF. Generation of B cell memory to the bacterial polysaccharide alpha-1,3 dextran. J Immunol. 2009; 183:6359–6368. [PubMed: 19841173]

12. Pritchard DG, Gray BM, Egan ML. Murine monoclonal antibodies to type Ib polysaccharide of group B streptococci bind to human milk oligosaccharides. Infect Immun. 1992; 60:1598–1602. [PubMed: 1548081]

13. Chen X, Martin F, Forbush KA, Perlmutter RM, Kearney JF. Evidence for selection of a population of multi-reactive B cells into the splenic marginal zone. Int Immunol. 1997; 9:27–41. [PubMed: 9043945]

14. Kearney JF, Barletta R, Quan ZS, Quintans J. Monoclonal vs. heterogeneous anti-H-8 antibodies in the analysis of the anti-phosphorylcholine response in BALB/c mice. European journal of immunology. 1981; 11:877–883. [PubMed: 7035186]

15. Bowman JC, Abruzzo GK, Anderson JW, Flattery AM, Gill CJ, Pikounis VB, Schmatz DM, Liberator PA, Douglas CM. Quantitative PCR assay to measure Aspergillus fumigatus burden in a murine model of disseminated aspergillosis: demonstration of efficacy of caspofungin acetate. Antimicrob Agents Chemother. 2001; 45:3474–3481. [PubMed: 11709327]

16. Kin NW, Stefanov EK, Dizon BL, Kearney JF. Antibodies generated against conserved antigens expressed by bacteria and allergen-bearing fungi suppress airway disease. J Immunol. 2012; 189:2246–2256. [PubMed: 22837487]

17. Jackson SL, Heath IB. Roles of calcium ions in hyphal tip growth. Microbiol Rev. 1993; 57:367–382. [PubMed: 8336672]

18. Hector RF, Yee E, Collins MS. Use of DBA/2N mice in models of systemic candidiasis and pulmonary and systemic aspergillosis. Infection and immunity. 1990; 58:1476–1478. [PubMed: 2323826]

19. Baker CJ, Rench MA, Fernandez M, Paoletti LC, Kasper DL, Edwards MS. Safety and immunogenicity of a bivalent group B streptococcal conjugate vaccine for serotypes II and III. The Journal of infectious diseases. 2003; 188:66–73. [PubMed: 12825173]

20. Alviano CS, Travassos LR, Schauer R. Sialic acids in fungi: a minireview. Glycoconj J. 1999; 16:545–554. [PubMed: 10815991]

21. Casadevall A, Pirofski LA. Antibody-mediated protection through cross-reactivity introduces a fungal heresy into immunological dogma. Infect Immun. 2007; 75:5074–5078. [PubMed: 17709417]
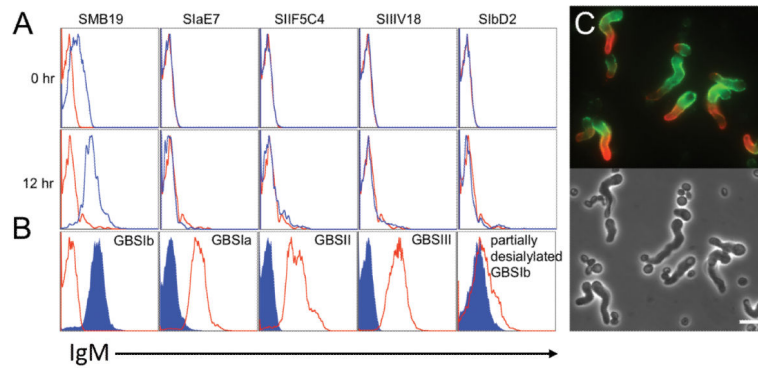
**Fig 1. The GBSIb type-specific mAb SMB19 binds to A.f.**
(A) Resting Conidia (0 hr) or Af hyphae from cultures (12 hr) were incubated with the indicated type specific anti-GBS mAbs (blue) or isotype control (red). Binding was visualized by Cy5-conjugated secondary anti-IgM antibody and analyzed by flow cytometry. (B) The indicated GBS serotypes were stained with SMB19 (blue) or the GBS type-specific IgM (red) followed by anti-IgM secondary and analyzed by flow cytometry. For the GBSIb serotype, SIaE7 (anti-GBSIa) was used as the control (red). (C) Fluorescence microphotograph (upper panel) and phase contrast (lower panel) of A.f. germlings following 9hrs of growth in RPMI media, EtOH fixation, and staining with SMB19 (red) and anti-α-1,3 glucan mAb A16 (green). White bar =10μm.
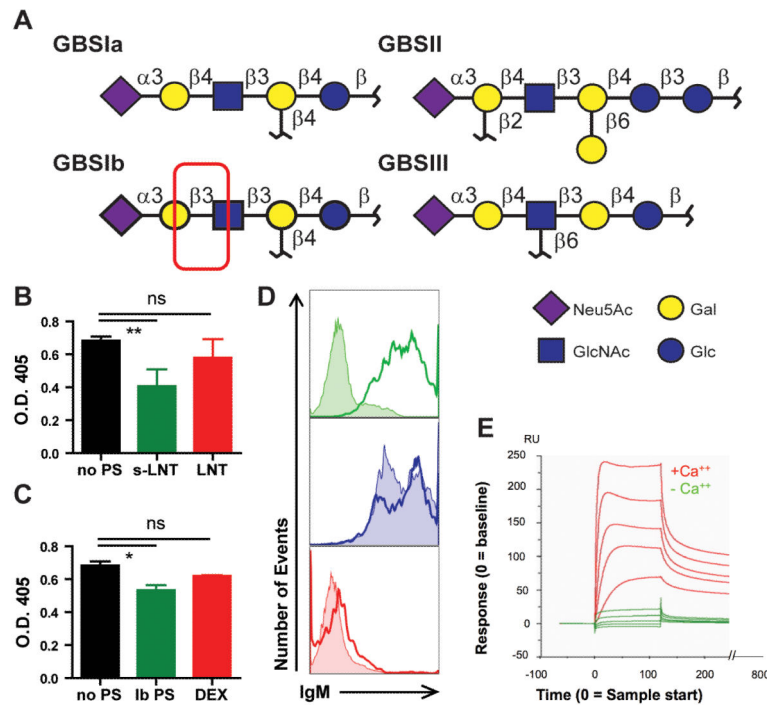
**Fig 2. SMB19 is highly specific for sLNT, is calcium dependent, and recognizes a PI-PLC sensitive epitope expressed by A.f.**

(A) The SMB19-reactive oligosaccharide expressed by GBSIb differs from other GBS capsular polysaccharides by a β1→3 instead of the more common β1→4 linkage. (B) Binding of SMB19 to A.f. visualized by ELISA assay. A.f. coated plates were incubated with SMB19 (black), SMB19 plus s-LNT (green), or SMB19 plus LNT (red) followed by an AP-labeled secondary antibody. (C) ELISA plates were coated with A.f. and incubated with SMB19 (black), SMB19 plus purified GBSIb polysaccharide (Ib PS, green), or SMB19 plus α-1,3 dextran (red) then with AP-labeled secondary antibody. SMB19 binding was analyzed by measuring the O.D. at 405 nm following development. Inhibition ELISAs were performed in triplicate and repeated twice with similar results. Data were analyzed One-way ANOVA with a Dunnett's post test, Overall ANOVA, P=0.0097, post-hoc, pair wise comparisons by Dunnett's test **= p<0.01. (D) Flow cytometric histograms of A.f. hyphae treated with PI-PLC (shaded histograms) or buffer treated (open histograms) were stained with SMB19 (green), SIbD2 (red), or the IgM anti-α-1,3 glucan mAb 1-21 (blue,), followed by secondary anti-mouse IgM-Cy5. Data were analyzed One-way ANOVA with a Dunnett's post test, Overall ANOVA, P=0.0524, post-hoc, pair wise comparisons by Dunnett's test*= p<0.05. (E) Surface plasmon resonance Biacore analysis of SMB19 binding in the presence or absence of $Ca^{+2}$. The vertical axis (RU) indicates mAb bound at multiple concentrations during 200 seconds of flow. Overlaid sensorgrams obtained with multiple concentration of SMB19 in the presence or absence of calcium are shown.
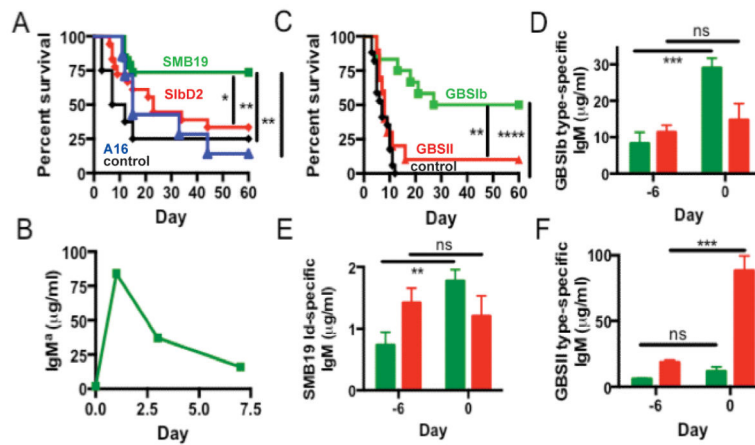
**Fig 3. Passive transfer of SMB19 or vaccination with GBSIb improves survival in a mouse model of disseminated I.A.**

(A) Survival of C57BL/6J mice passively transferred with 200 μg SMB19 (green, n=19), SIbD2 (red, n=18), A16 (blue, n=7), or PBS (black, n=8) i.p. immediately before i.v. infection with $2 \times LD_{50}$ ($2 \times 10^6$) A.f. conidia. Results were pooled from 3 separate experiments. Asterisks denote significant differences in average survival compared to mice administered SIbD2, A16, or PBS. (B) Serum IgM[a] levels were analyzed at various times before and after passive transfer of 200 μg SMB19 by ELISA. (C) Survival of mice vaccinated i.v. with GBSIb (green, n=12), GBSII (red, n=10), or PBS (black, n=17) 6 days before i.v. infection with A.f. Results are pooled from 2 separate experiments with similar results. Asterisks denote significant differences in average survival of GBSIb vaccinated animals compared with GBSII vaccinated and PBS control groups. (D-F) Serum GBSIb type-specific IgM (D), SMB19 idiotype-positive IgM(E), and GBSII type-specific IgM (F) quantified by ELISA immediately before (Day -6) or 6 days after (Day 0) vaccination with GBSIb (green) or GBSII (red). Asterisks denote significant differences between serum IgM levels at day -6 and day 0. Data were analyzed by a two-tailed unpaired t test, *=p<0.05; **= p<0.01; ***= p<0.001; ****= p<0.0001. In survival studies, statistical significance was determined by log rank test.
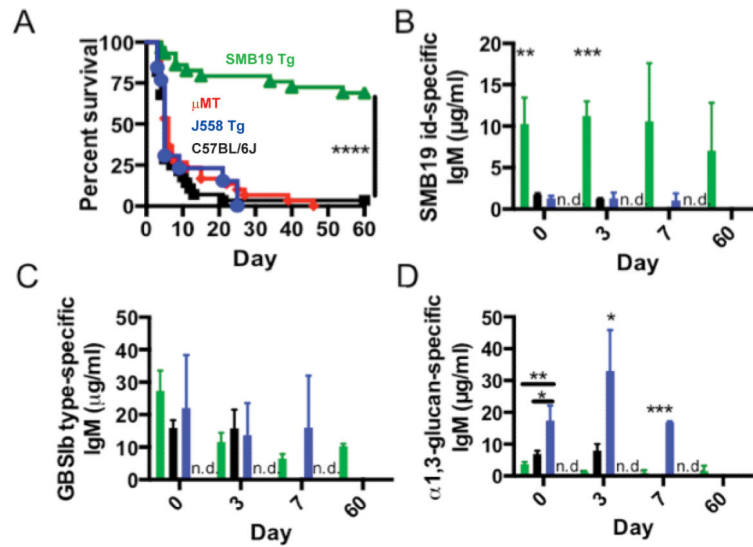
**Fig 4. SMB19 Tg mice are protected in a mouse model of disseminated I.A.**

(A) Survival of C57BL/6J (black, n=27), µMT (red, n=30), J558 Tg (blue, n=13) or SMB19 Tg mice (green, n=29) infected with A.f. i.v. Results are pooled from 3 experiments with similar results. Asterisks denote significant differences in average survival rate of SMB19 Tg mice compared to J558 Tg, µMT, and C57BL/6J groups. (B-D) Serum concentration of SMB19 idiotype-specific IgM(B), GBSIb type-specific IgM (C), or anti-α-1,3 glucan-specific IgM (D) in C57BL/6J, SMB19 Tg, J558 Tg, or µMT mice at various time points after i.v. infection with A.f. n=3 / group. Bar colors correspond to mouse genotypes in Fig 5A. No serum antibodies were detected in µMT mice (n.d., red bars). Results are representative of 2 independent experiments with similar results. Asterisks denote significant differences in serum antibody levels between mouse groups at various time points. Data was analyzed using a One-way ANOVA with a Tukey's post test. In survival studies, statistical significance was determined by log rank test, *= $p<0.05$, **= $p<0.0$, ***= $p<0.001$, ****; $p<0.0001$.
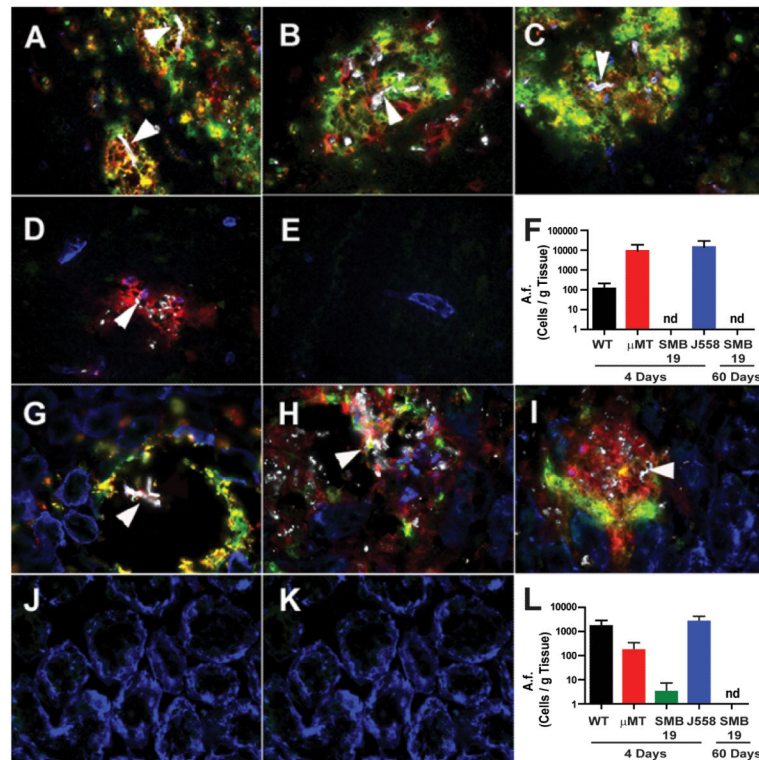
**Fig 5. SMB19 Tg mice have low or undectable A.f. fungal burden in their targeted tissues following A.f. challenge**

(A-E) Immunofluorescence analysis on frozen sections of cerebrum from C57BL/6J (A), μMT mice (B) J558 Tg (C) mice 4 days following i.v. infection with A.f. compared to SMB19 Tg at 4 days (D), or 60 days (E). (G-K) Analysis of kidney tissue from C57BL/6J (G), μMT mice (H), J558 Tg (I) compared to SMB19 Tg at 4 days (J) and 60 days (K) after i.v. infection with A.f. Sections are stained with anti-MAC1 (red), anti-Ly6G (green), anti-β-1,3 glucan (white), and anti-laminin (blue). White arrows indicate morphologically distinct hyphae in tissues from WT C57BL/6J, μMT and J558 Tg mice or anti-β-1-3 glucan remnants in SMB19 treated mice. (F, L) Quantitative PCR analysis of fungal burden in brain (F) or kidney (L) of WT C57BL/6J (black), μMT (red), SMB19 Tg (green), and J558 Tg (blue) mice at the indicated times after infection with A.f. Data represent the mean + SEM from 2 independent experiments with 3 mice per group. nd= not detectable. The Y axis represents the number of A.f. conidial equivalents per g of infected tissue extrapolated from cycle threshold calibration curves generated by the inclusion of known numbers of A.f. conidia into naive tissue preparations.
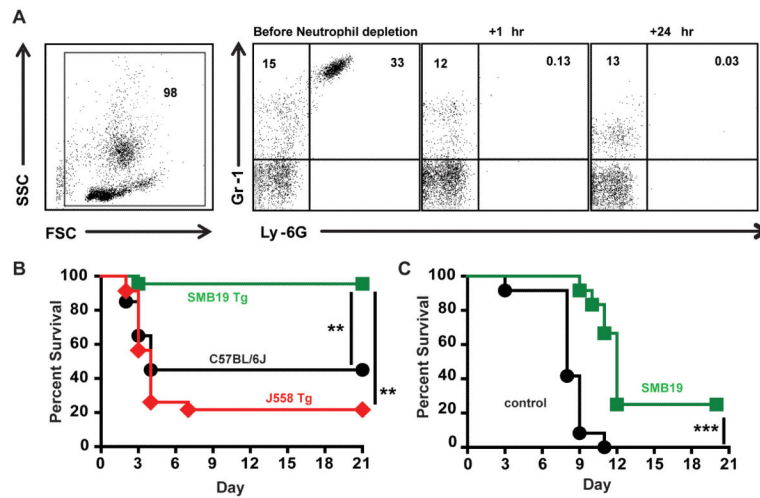
**Fig 6. Neutrophil depleted SMB19 Tg mice and Ncf1$^{m1J}$/J mice co-administered i.t. with SMB19 are protected after i.t. A.f infection**

(A) Flow cytometric analysis of peripheral blood neutrophil frequencies in mice before or at the indicated times following the i.p. administration of 200 μg anti-Ly6G. (B) Survival of transiently neutropenic SMB19 BCR Tg (green, n=21), J558 BCR Tg (red, n=21) and WT C57BL/6J mice (black, n=20) administered anti-Ly6G 1 day before i.t. infection with 2.5×10$^7$ A.f. conidia. (D) Survival of Ncf1$^{m1J}$/J mice challenged i.t. with 1×10$^5$ A.f. conidia alone (black) or in combination with 50μg of SMB19 (green). Results are pooled from two independent experiments and include 12 mice per group. Statistical analysis was performed using the Mantel-Cox Log-rank test.